Sea Level Changes Detected by Using Satellite Altimeter Data and Comparing with Tide Gauge Records in China Sea

Zhengtao Wang Jiancheng Li Dingbo Chao
School of Geodesy and Geomatics, Wuhan University 129 Luoyu Road, Wuhan 430079, China
zhli@wtusm.edu.cn

Jianguo Hu
China Academy of Surveying and Mapping 16 Beitaiping Road, Beijing 100039, China

Abstract. The Topex/Poseidon (cycles 9-249), Geosat/ERM and ERS-2 (cycles 0-44) altimeter data are used to analyze the sea level changes in China Sea. The sea level changes in studying areas derived respectively from TOPEX/Poseidon and ERS-2 data during the same period are almost coincident with each other. The results are compared with the tide gauge records at different sites of China Sea, and they indicate that the sea level change in China Sea appears to be a rising trend with 2~3 mm per year. Moreover, the trends of the seasonal sea level changes of this region are reverse to that of the global sea. We also investigate some possible implied relationships of local sea level changes to some anomalies of sea surface heights due to such as El Niño/La Niña phenomena in different time and spatial spans.

Keywords. Sea-level change, Altimeter, Tide gauge

1 Introduction

The ocean is one of the important parts of global weather system. The variations of global mean sea level are one of the important indicators of global climate changes. It can directly affect global weather and long period climate evolvement. The sea level changes are caused by seasonal sea warming, colding, winds and all kinds of non-conservative forces which act on the sea level.

Altimeter data of high spatial resolution and long period temporal coverage provide a broad band of information about sea level variation. The time sequence of sea level heights above a reference ellipsoid can be obtained from the altimeter data and they can give the analysis bases for global weather change and El Niño and La Niña events indicated by sea level changes.

Since Kaula put forward altimeter technical conception in 1969, satellite altimeters have acquired numerous altimeter data during more than two decades, and the altimeter technical is becoming more maturity. The sequence of 15 years observation data of different satellites, including NOAA Geosat GM (1985.3-1986.9), ERM (1986.9-1989.12), ERS-1 (1991.8-1996.4), ERS-2 (1995.4-2000.12) and T/P data from 1992.8 have widely been used in geophysical studies.

Satellite altimeter has revolution fionized the mapping of the ocean surface of the Earth in terms of sampling frequency and observational accuracy (Yuchan Yi, 1995). Geosat data released in 1997 have a observable amelioration in orbit determination by using the Doppler tracking data and JGM-3 gravity field model. Geosat orbit precision was improved from 2-3 meter reducing to 0.1 meter. In despite of PRARE tracking system invalid, ERS-1's orbit precision still reaches 0.15 meter, and ERS-2's one is better than 0.1 meter as well as T/P satellite' orbit precision reaches 0.035 meter because of a GPS receiver on board, equipped Laser retroreflector array (LRA) and double-frequency radar altimeter with the precision of 0.032 meter.

Altimeter can provide a dense time sequence of global sea surface height (SSH) observation with high repetition, which is new information useful for inspecting the temporal variation of SSH. In this study, three types of satellite data (T/P GDRs (cycles 9 to 249), ERS-2 GDRs(cycles 0 to 44) and complete Geosat/ERM will be used to analyse and investigate the global and local sea level changes.

2 Mathematical Models

2.1 Collinear Analyses

International Association of Geodesy Symposia, Vol. 126
C Hwang, CK Shum, JC Li (eds.), International Workshop on Satellite Altimetry

Altimeter satellite orbits were usually designed in repeated ones. Accordingly, the ground tracks on the Earth surface should be strictly repeated. However, because all kinds of non-gravitational perturbing forces such as air drag and solar radiation pressure act on satellites, the ground tracks of the corresponding repeat cycles don't exactly coincide with each other, but they drift within a few kilometres wide. For most conditions, two adjacent tracks are nearly parallel arcs (see figure 1). In collinear analysis, we choose one track as a reference track to be fixed, and then determine the longitude and SSH of the same latitude point on other collinear arcs.

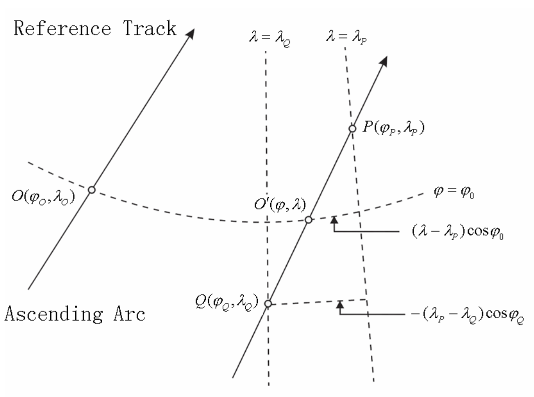

Fig. 1a Ascending Arc Collinear

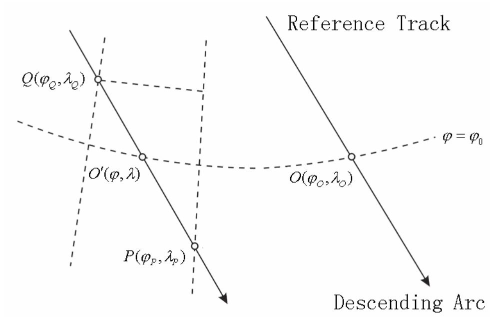

Fig. 1b Descending Arc Collinear

For ascending arcs (see figure 1a, here inclination i<90º), point O(φ_0, λ_0) is an observation point on the reference track, and O'(φ, λ) is the point with the same latitude of point O on a collinear arc. In generally, point O' would not be an observation point on the track. Therefore, the sea surface height of point O' should be computed using linear interpolation in terms of its two neighboring actual observation points P(φ_P, λ_P) and Q(φ_Q, λ_Q).
The longitude of O' can be interpolated by

$$\lambda = \lambda_P - D_1(\varphi_P - \varphi_O)/\cos\varphi_O \quad (1)$$

Where

$$D_1 = (\lambda_P - \lambda_Q)\cos\varphi_Q/(\varphi_P - \varphi_Q) \quad (2)$$

For descending arcs, (see figure 1b, i<90º), the interpolation formula of the longitude is

$$\lambda = \lambda_P - D_2(\varphi_O - \varphi_P)/\cos\varphi_O \quad (3)$$

Where

$$D_2 = (\lambda_P - \lambda_Q)\cos\varphi_Q/(\varphi_Q - \varphi_P) \quad (4)$$

In another conditions, i.e when inclination is larger than 90 degree (i>90º), the similar formula for interpolating the longitude are:
for ascending arc

$$\lambda = \lambda_P + D_1(\varphi_P - \varphi_O)/\cos\varphi_O \quad (5)$$

$$D_1 = -(\lambda_P - \lambda_Q)\cos\varphi_Q/(\varphi_P - \varphi_Q) \quad (6)$$

and for descending arc

$$\lambda = \lambda_P + D_2(\varphi_O - \varphi_Q)/\cos\varphi_O \quad (7)$$

$$D_2 = (\lambda_P - \lambda_Q)\cos\varphi_Q/(\varphi_P - \varphi_Q) \quad (8)$$

After the position of the point O'(φ, λ) is determined, its SSH can be calculated by the following linear interpolation formula.

$$H = H_Q + (H_P - H_Q)\frac{(\varphi_O - \varphi_Q)}{(\varphi_P - \varphi_Q)} \quad (9)$$

2.2 Inverse Barometer Correction

Atmospheric pressure variations are the most important excitation sources of sea level changes. The Inverse Barometer solution depends approximately on the oceanic response to fluctuations in atmospheric pressure.
The standard Inverse Barometer Correction IB is given by the equation:

$$IB = -10.1(P - 1013.3)\ \text{(mm)} \tag{10}$$

Where P is atmospheric pressure; 1013.3 mbar is standard atmosphere pressure.
The equation (10) assumes that sea level changes are proportional to the difference between real-time atmosphere pressure and standard atmosphere pressure.
Rapp (1994) suggested that standard atmosphere pressure should be replaced by average atmosphere pressure of one cycle, so

$$\overline{IB} = -10.1(P - \overline{P}) \tag{11}$$

Where $\overline{P}$ is average atmosphere of one cycle.
The differences between IB computed eq.(10) and $\overline{IB}$ computed by eq.(11) are –5mm to 47mm for T/P data, -6mm to 26mm for ERS-2 data and –25mm to 36mm for Geosat/ERM data respectively.
Figure 2, 3, 4 show the performance of the differences versus cycles for T/P, ERS-2 and Geosat/ERM respectively. In the figures, the largest differences are plotted as a thick solid line and the minimum differences are plotted as a thin broken line.

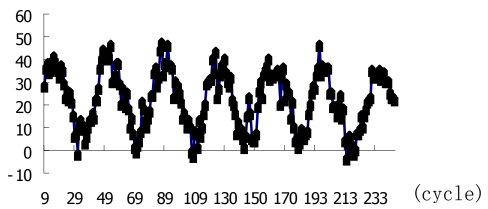

Fig. 2 The Differences between *IB* and $\overline{IB}$ Versus the Repeated Cycles for T/P Data

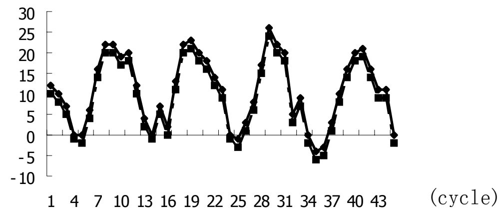

Fig. 3 The Differences between *IB* and $\overline{IB}$ Versus the Repeated Cycles for ERS-2 Data

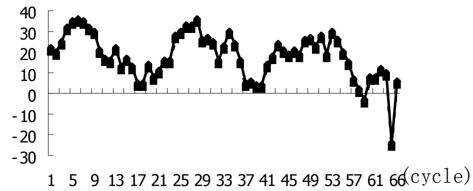

Fig. 4 The Differences between *IB* and $\overline{IB}$ Versus the Repeated Cycles for Geosat/ERM Data

2.3 Computation of Sea Level Change

The altimeter observation of the instantaneous sea surface height h^a above a reference ellipsoid surface is described in terms of the geoid height N, the stationary sea surface topography ζ_0, the temporal variation of sea surface topography ζ_t and the altimeteric error ε by

$$h^a = N + \zeta_0 + \zeta_t + \varepsilon \tag{12}$$

We assume that the geoid height and the stationary sea surface topography do not change with time, and sea level changes only have a few centimeters order of magnitude. Hence, Mean Sea level Variation (MSLV) can be detected from altimeteric data after eliminating mean sea level affection in sea height through collinear analyses.
The computation of MSLV along collinear tracks is performed in a collinear analysis for each set of collinear tracks using the following procedure:

1. A set of reference tracks called collinear datum tracks determined by more observations and higher precision are determined. They can represent the repeated tracks of satellite.
2. Sea surface height, longitude are interpolated at the same latitude of other cycle collinear tracks relative to reference tracks using collinear analysis equations (1)-(9) and farther sea level change are computed.

3. MSLVs of month, season and year in different area are computed using the computed sea level height and change values in a collinear analysis.

2.4 Tide Gauge Records Processing

Annual tide gauge records of 29 stations along the coastal of China covering the past 50 years (1950-1999) are used in this study. An annual sea level changes around a tide station can be obtained by subtracting the mean value of the annual MSLs of 50 years from the annual MSL of each year over the local area of the station, and the results for 6 stations (Tanggu, Yantai, Xiamen, Beihai, Lianyungang, Kanmen) are shown in figure 5. The annual mean sea level variations of the whole China sea are can then be computed by subtracting the MSL of 50 years of all stations from the MSL of each year of the area, and the results are shown in figure 6. The expression of annual MSLV is as follows

$$MSLV_i = \left(\sum_{j=1}^{m} a(i,j)\right)/m - \left\{\sum_{i=1}^{n}\left[\left(\sum_{j=1}^{m} a(i,j)\right)/m\right]\right\}/n \quad (13)$$

Where a(i,j) is the real tide record (annual MSL), and i denotes year as well as j stands for tide station. Here n=50 and m=29.

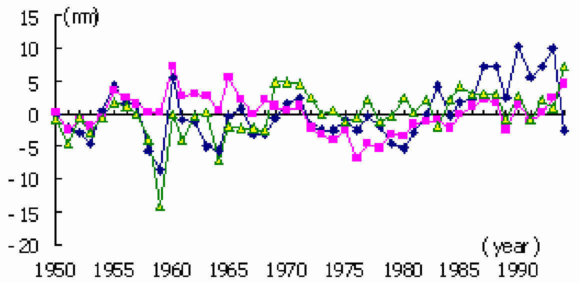

a

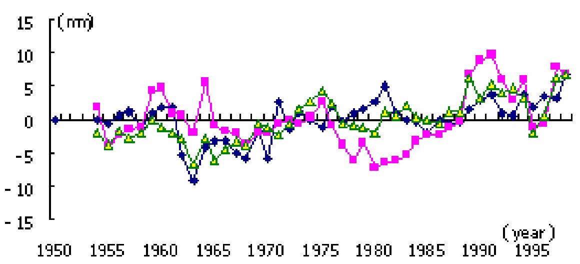

b

Fig. 5 Annual Sea Level Variations Determined from Tide Records in Different Station Areas

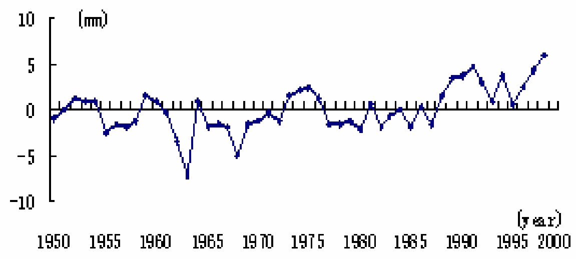

Fig. 6 Annual Sea Level Variations Determined from Tide Records of 29 Stations in China Sea

3 Altimeter Data Description and Editing

The Geosat/ERM of 17-day repeat data which released in 1997 are used for this study. This data set of GDR data based on the newest JGM-3 orbits distributed by NOAA. The corrections for the solid earth tide, the ocean tide, wet tropospheric component and dry tropospheric component were applied to the SSHs data.

The editing (deleting) criteria of Geosat/ERM data were devised with reference to the OSU recommend data editing criteria, and one-per-second SSH data sampling points of individual Geosat GDR cycles were
edited using the following criteria:

a. σ <0 orσ>10cm. Standard deviation from a linear fit to the 10 per second SSH values used to compute one-per-second SSH;
b. SWH<-0.5m or SWH>1.0m;
c. Standard deviation of SWH<0.1m;
d. Attitude angle >1.3 degree;
e. Ocean tide correction exceeds 1m
f. Any of flag bit 2, 3, 4, 5, 6, 7, 8=1;
g. Flag bit 0=0 and SSH=0;
h. Maximum difference between 10 per second and one-per-second SSH exceeds 1m;
i. The difference between SSH after correcting and mean SSH of OSU95 exceeds 1m.

All standard geophysical correction applied come from handbook (NOAA, 1997) except for electro-magnetism departure corrections in which 2% of SWH was adopted (Cheney, et. Al, 1987, Denker and Rapp, 1990). The IB correction with respect to an average atmosphere pressure of each cycle was applied to the SSH data.

The Topex/Poseidon data used in this study were obtained from the newest third version GDR of AVISO. The editing deleting criteria were taken from handbook of AVISO and that of OSU (Rapp, 1994) and they are as follows:

a. |Δ| > 1, where Δ is the difference between the corrected SSH and Mean SSH of OSU95, and SWH ≥ 9m;
b. 3≤ |Δ| ≤5m and SWH_RMS > 4m;
c. |Δ| ≥ 5m.

The geophysical corrections include dry tropospheric, wet troposphric, ionospheric correction, oceanic state (k1) correction and ocean tide (CSR3.0 model), solid tide and pole tide correction.

In the ERS-2 editing procedure, a data point will be deleted under the following conditions according to its handbook:

a. Manoeuvre flag;
b. Radiometer land flag;
c. Ice flag;
d. SSH> 100m or SSH< -130m;
e. Number of 20-Hz measurements< 10;
f. Standard deviation on 20-Hz measurements< 0 or > 450cm;
g. Dry tropospheric correction< -2500mm or > -1900mm;
h. Radiometer wet tropospheric correction < -500mm or > -1mm;
i. Ionospheric correction < -200mm or > -1mm;
j. SWH<0 or >10m;
k. Sigma naught <6dB or >30dB;
l. Ocean tide correction <-5000mm or >5000mm;
m. Solid earth tide correction < -1000mm or > 1000mm.

Using the above criteria, not only useless data over land, ice or larger inland lakes but also the data containing the gross errors of altimeteric measurements are deleted. In other words, these criteria and all types of geophysical corrections applied in data editing an processing will assume all data to be used with higher qualities, i.e, higher accuracy and reliability.

4 Results and Analysis

In order to study the annual MSLV of global and China sea and adjacent sea areas (0°N~40°N, 100°E~145°E). We made the respective collinear analysis processing for the repeated track altimeter data of per year including T/P data starting with the eleventh cycle, Geosat/ERM starting with the forth cycle. Fig. 7 and 8 show the analysing results of the annual MSLV. For studying the seasonal MSLV, the collinear analysises are made for T/P data of every 10 segment cycles, ERS-2 data of every 3 segment cycles and Geosat data of every 6 segment cycles. Consequently, the global and local MSLVs are detected, and the results are shown in Fig. 9 ~Fig. 15 below.

Fig. 7 and Fig. 8 indicate the MSLVs trends of China sea and global ocean determined using 5 years (1993-1998) T/P data, which show that the trends of each year of China sea would be different from that of global ocean, and also show that the trend of each year is not consistent with each other for both China sea and global ocean. From Fig. 7, it indicates that the sea level change in China Sea appears to be a rising trend with 2~3 mm per year. China sea and global ocean appear to have the same MSLV trends during 1993-1996, while they have the inverse MSLV trends during 1997-1998, i.e, the sea level of China Sea was rising, and that of global ocean was falling within these two years.

Fig. 9 and Fig. 10 show that the seasonal MSLVs implied by T/P and ERS-2 data respectively have almost the same trends during the same period, that is, the sea level appears to rise in the first and last seasons of each year, while to fall in the second and third seasons in China sea, especially, the amounts of the third and forth MSLVs are very close to each other.

From Fig. 11-13, they show that the trend of the global sea level changes have an apparent correlation with seasonal alternation, i.e, it is rising during the first and last seasons of each year, and falling during the second and third seasons, especially, the falling trend is very significant in the second season. To testify whether it is correct or not to determine sea level variation by satellite altimeter, this paper uses the data of tide stations for an external check. The results calculated by satellite altimeter data are compared with those resulting from the data of tide stations and it shows that the trends of both results are in complete consistence.

In the offing of China, the sea level falls in spring and winter and rises in summer and autumn with distinct regularity. It turns out that using satellite altimeter data to analyse the long-term variation of sea level is a low-cost and effective method.

Finally, to investigate the correlative relation between the abnormal variation of sea level and El Niño and La Niña phenomena, we analysed the sea level variation of east equator Pacific using altimeter data. When El Niño and La Niña phenomena occur in 1992~1993 and in 1997~1998, as shown in Fig. 14~16, the phases of MSLVs are reverse to those of the offing of China (west equator Pacific area). In east Pacific, the sea level rises in spring and winter and falls in summer and autumn. These facts would be the possible characteristics of El Niño and La Niña events.

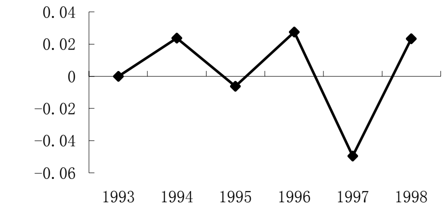

Fig. 7 Annual MSLVs (m) of China Sea from T/P

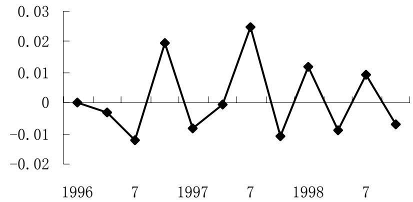

Fig. 12 Seasonal MSLVs (m) of Global Sea from ERS2

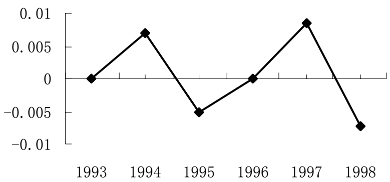

Fig. 8 Annual MSLVs (m) of Global Sea from T/P

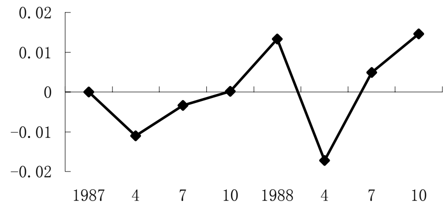

Fig. 13 Seasonal MSLVs (m) of Global Sea from Geosat/ERM

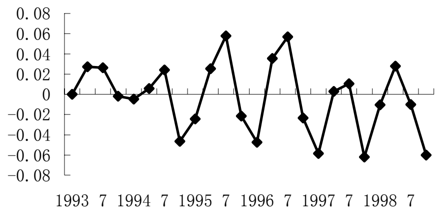

Fig. 9 Seasonal MSLVs (m) of China Sea from T/P

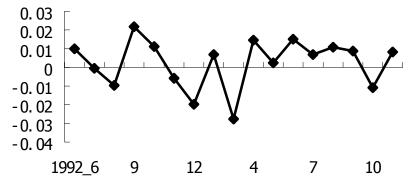

Fig. 14 Monthly MSLVs (m) of Eastern Equatorial from ERS

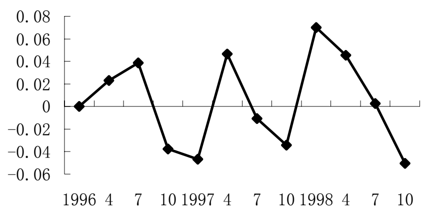

Fig. 10 Seasonal MSLVs (m) of China Sea from ERS-2

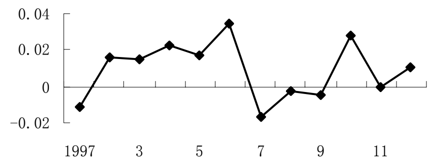

Fig. 15 Monthly MSLVs (m) of Eastern Equatorial from T/P

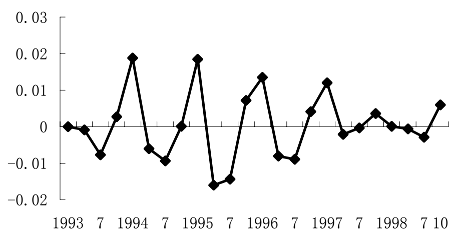

Fig. 11 Seasonal MSLVs (m) of Global Sea from T/P

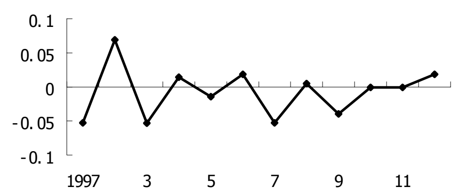

Fig. 16 Monthly MSLVs (m) of China Sea from T/P

Acknowledgments. This work has received support from National Natural Science Foundation Council grants 40274004 and 49625408. We are very grateful to ESA for ERS-1 and ERS-2 altimeter data, NOAA for Geosat data and CNES for Topex/Poseidon data.

References

AVISO. (1996). Aviso User Handbook: Merged TOPEX/POSEIDON Products (Gdr-Ms), AVI-NT-02-101-CN, Edit.3.0.

Brenner, A. C., C. J. Koblinsky and B.D. Beckey (1990). A Preliminary Estimated of Geoid-Induced Variations in Repeat Orbit Satellite Altimeter Observations, J Geophys Res, 95, pp. 3033-3040.

Callahan, P. S. (1993). TOPEX/POSEIDON NASA GDR Users Handbook, JPL rep D-8590, rev C.

Chen, J. L., C. Shum, C. Wilson and D. Chamber (2000). Seasonal Sea Level Change from TOPEX/POSEIDON Observation and Thermal Contribution, J Geod, 73, pp. 323-332.

Chen, J. L., C. R. Wilson, D. P. Chambers, R. S. Nerem and B. D. Tapley (1998a). Seasonal Global Water Mass Balance and Mean Sea Level Variations, Geophys Res Lett, 25, pp. 3555-3558.

Chen, Z. Y., A. L. Ye and J. C. Zuo (1995). Advances in Ocean Tide Research over the Past 40 Years in China, Journal of Ocean University of Qingdao, 10, pp. 435-444.

Cheney, R. E., B. C. Douglas, R. W. Agreen, L. Miller, D. L. Porter and N. S. Doyle (1987). Geosat Altimeter Geophysical Data Records-User Handbook, NOS NGS-46, Noaa Tech Memo, Natl. Ocean Serv., Natl. Geod. Surv., Rockville, Md.

Denker, H., and R. H. Rapp. (1991). Geodetic and Oceanographic Results from the Analysis of 1 Year of Geosat Data, J Geophys Res, 95, pp. 13151-13168.

Dickman, S. (1988). Theoretical Investigation of the Oceanic Inverted Barometer Response, J Geophys Res, 93, pp. 14941-14946.

Douglas, B. (1996). Global Sea Level Rise, J Geophys Res, 96, pp. 6981-6992.

Fu, L. L., and R. A. Davidson (1995). A Note on Barotropic Response of Sea Level to Time-Dependent Wind Forcing, J Geophys Res, 100, pp. 24955-24963.

Ma, J., Q. Zhang and X. Chai. (1996). Rising Trend of Relative Sea Level along the Coast of East Asia, Mar Geod, 19, pp. 257-268.

Minster, J. F., A. Cazenave, V. Serafini, M. C. Gennero and P. Rogel (1999). Annual Cycle in Mean Sea Level from TOPEX/POSEIDON and ERS-1: Inference on the Global Hydrological Cycle, Global Planet Change, 20, pp. 57-66.

Minster, J. F., C. Brossier and P. Rogel (1995). Variation of the Mean Sea Level from TOPEX/POSIEDON Data, J Geophys Res, 100, pp. 25153-25161.

Nerem, R. S. (1995). Measuring Global Mean Sea Level Variations Using TOPEX/POSEIDON Data, J Geophys Res, 100, pp. 25135-25151.

NOAA. (1997). The Geosat Altimeter JGM-3 GDRs on CD-ROM. NODC Laboratory for Satellite Altimetry.

Raofi, B. (1998). Ocean's Response to Atmosphere Pressure Loading: the Inverted Barometer Approximation for Altimetric Measurements, PHD Diss, The University of Texas at Austin.

Rapp, R. H., Y. C. Yi and Y. M. Wang. (1994). Mean Sea Surface and Geoid Gradient Comparisons with TOPEX Data, J Geophys Res, 99, pp. 24657-24667.

Repert, J. P., J. R. Donguy, G. Elden and K. Wyrtki (1985) Relations between Sea Level, Thermocline Depth, Heat Content, and Dynamic Height in the Tropical Pacific Ocean, J Geophys Res, 90, pp. 11719-11725.

Wyrtki, K. (1985). Water Displacements in the Pacific and Genesis of El Niño Cycles, J of Geophys Res, 90, pp. 7129-7132.

Yi, Y. C. (1995). Determination of Gridded Mead Sea Surface from TOPEX, ERS-1 and Geosat Altimeter Data, Rep. 434, Dept. of Geodetic Science and Surveying, The Ohio State University, Columbus.